nature COMMUNICATIONS

ARTICLE

Received 22 Oct 2013 | Accepted 18 Dec 2013 | Published 16 Jan 2014

DOI: 10.1038/ncomms4153

Kctd10 regulates heart morphogenesis by repressing the transcriptional activity of Tbx5a in zebrafish

Xiangjun Tong[1,*], Yao Zu[1,*], Zengpeng Li[2,*], Wenyuan Li[1], Lingxiao Ying[1], Jing Yang[1], Xin Wang[1], Shuonan He[1], Da Liu[1], Zuoyan Zhu[1], Jianming Chen[2], Shuo Lin[3] & Bo Zhang[1]

The T-box transcription factor Tbx5 (Tbx5a in zebrafish) plays a crucial role in the formation of cardiac chambers in a dose-dependent manner. Its deregulation leads to congenital heart disease. However, little is known regarding its regulation. Here we isolate a zebrafish mutant with heart malformations, called *34c*. The affected gene is identified as *kctd10*, a member of the potassium channel tetramerization domain (KCTD)-containing family. In the mutant, the expressions of the atrioventricular canal marker genes, such as *tbx2b*, *hyaluronan synthase 2* (*has2*), *notch1b* and *bmp4*, are changed. The knockdown of *tbx5* rescues the ectopic expression of *has2*, and knockdown of either *tbx5a* or *has2* alleviates the heart defects. We show that Kctd10 directly binds to Tbx5 to repress its transcriptional activity. Our results reveal a new essential factor for cardiac development and suggest that *KCTD10* could be considered as a new causative gene of congenital heart disease.

[1] Key Laboratory of Cell Proliferation and Differentiation of Ministry of Education, College of Life Sciences, Peking University, Beijing 100871, PR China. [2] State Key Laboratory Breeding Base of Marine Genetic Resources, Third Institute of Oceanography, State Oceanic Administration, 184 University Road, Xiamen 361005, Fujian Province, PR China. [3] Department of Molecular, Cell and Developmental Biology, University of California Los Angeles, Los Angeles, California 90095-1606, USA. * These authors contributed equally to this work. Correspondence and requests for materials should be addressed to X.T. (email: xiangjuntong@pku.edu.cn).

During the development of the vertebrate embryo, the heart is the earliest organ to form and to function. The primitive heart is a simple tube containing only two layers: an outer myocardium and an inner endocardium. Cardiac jelly is localized between the two layers and occupies the majority of the wall of the heart tube[1]. Subsequently, the tube undergoes a series of complicated morphogenetic processes called heart looping to form the final multi-chambered heart[2]. The formation of the atrioventricular canal (AVC) is one of the most important steps. The AVC separates the linear heart tube into the initial atrial and ventricular chambers and the myocardial cells at the AVC proliferate slowly and retain a slow conduction velocity, which is critical for the establishment of synchronized beating in the embryonic heart[3].

In the last 20 years, several signalling pathways that control cardiac development have been identified in vertebrates, ranging from zebrafish to humans. All these signalling pathways guide cardiogenesis through a series of transcription factors, such as the GATA family, NK2 transcription factor-related 5 (Nkx2-5), the basic helix-loop-helix transcription factors dHand and MesP1, Kruppel-like factor, the T-box (Tbx) transcription factors and FoxN4 (refs 4–8).

The critical roles of the T-box transcription factors are initially revealed by analysing the phenotypes of human congenital heart malformations. For example, *TBX1* haploinsufficiency causes DiGeorge syndrome and *TBX5* haploinsufficiency results in Holt-Oram syndrome[9,10]. Targeted mutagenesis or knockdown of the genes encoding the T-box transcription factors demonstrates that Tbx1, Tbx2, Tbx3, Tbx5 (Tbx5a in zebrafish), Tbx18 and Tbx20 play essential roles during cardiac development in the mice or zebrafish[11–19].

Tbx5 plays a crucial role in the formation of the cardiac chambers and the AVC. This protein synergistically acts with Tbx20, BMP4, GATA4, Nkx2-5 and other factors to regulate the expression of many chamber-specific genes[8,14,20]. It also restricts the expression of *Tbx2* (*tbx2b* in zebrafish) and *has2* (hyaluronan synthase 2) at the AVC to facilitate the formation of the endocardial cushion and valve[21]. Deregulation of *has2* abrogates the normal cardiac morphogenesis[22,23].

Abnormal cardiac morphogenesis is closely correlated with the dose of Tbx5 (refs 24,25). Holt-Oram syndrome occurs in heterozygous individuals, whereas homozygous-null mutations in *Tbx5* exhibit very severe heart malformations. *Tbx5* duplication or overexpression results in phenotypes similar to the Holt-Oram syndrome[26]. These data indicate that the expression level and/or the activity of Tbx5 are precisely controlled during heart development. However, the mechanism of the regulation of Tbx5 is poorly understood.

In this study, we isolate a zebrafish mutant with heart malformations, called *34c*. On the basis of positional cloning, the affected gene is identified as *kctd10*, a member of the potassium channel tetramerization domain (KCTD) containing family. KCTD proteins comprise a large family containing at least 22 members in human, but only several members have been studied. Because *KCTD* genes have not been targeted in any model organisms, their precise roles in development are unknown. Here we demonstrate that Kctd10 protein controls cardiac development by directly binding to Tbx5 to repress its transcriptional activity. Therefore, Kctd10 plays an essential role in cardiac development, which could be considered as a new candidate for the genetic screening of congenital heart diseases in the future.

Results

***kctd10* deficiency leads to heart defects in the mutant *34c*.** We identified a spontaneous recessive mutation called *34c* that disrupted cardiac function in zebrafish. This mutant exhibited AVC malformations and heart looping failure. The mutants were indistinguishable from their siblings until ~36 hpf (hours post fertilization), when heart looping starts[8,27]. Thereafter, approximately one-fourth of the embryos displayed heart looping defects, then weakened heart contractility, weakening circulation, an accumulation of blood cells in the venous sinus, and pericardial oedema at 48 hpf (Fig. 1a,b). The hearts of their wild-type siblings beat normally at 48 hpf (Supplementary Movie 1). In contrast, the atrium of the *34c* mutant appeared to have very weak contractility and a slower heart rate. However, global contraction still occurred and no fibrillation or arrhythmia was observed. The ventricle became completely still at 48 ~ 52 hpf (Supplementary Movie 2).

In the mutant embryos at 36 hpf, no marked differences were observed when compared with wild-type, but the mutants had markedly smaller eyes and smaller heads at 48 hpf (Fig. 1a,b; supplementary Fig. 1a–d). Moreover, the pectoral fins of the mutant larvae were smaller than their normal siblings (Supplementary Fig. 1e–j).

To further investigate the cardiac malformations, we analysed the *34c* mutant under the backgrounds of two transgenic fish lines: *Tg*(*cmlc2:EGFP*) that labels the myocardium, and *Tg*(*flk:mCherry*) that labels the endocardium. As visualized using these transgenic lines, both the myocardium and the endocardium of the chambers in the mutants were markedly shrunken and the heart failed to loop normally compared with the wild-type siblings (Fig. 1c–h). The endocardium was more severely reduced than the myocardium, with nearly no lumen present (Fig. 1g,h). The defect became increasingly severe over time. The oedema of the venous sinus appeared at 50 hpf and the mutant died at ~5 dpf (days post fertilization). However, the patterns of blood vessels in the mutants were indistinguishable from that in the wild-type siblings (Supplementary Fig. 2).

We performed positional cloning to identify the affected gene that caused the phenotype of *34c*. Meiotic mapping of *34c* identified a 0.63-Mb interval between rs40961672 (LG (linkage group) 5: 21 468 103 bp) and Z10456 (LG5: 20838789–20838997 bp) of chromosome 5 (Fig. 1l). The annotated Ensembl zebrafish genome assembly Zv9 suggested 10 candidate genes in this region. After sequencing the coding region of these candidate genes, a homozygous A-to-T substitution at position 120 of exon 2 of the gene *kctd10* was identified in the *34c* mutants (Fig. 1m). This change replaced Lysine (AAG) with a pre-mature stop codon (TAG) at amino-acid position 113. The tetramerization domain of Kctd10 is located within its N-terminus, and the truncation by the nonsense mutation eliminates part of this domain. When we in-crossed the $kctd10^{+/-}$ fish, it always resulted in 25% of the embryos displaying the mutant phenotype. No obvious dominant-negative activity was observed.

To confirm that the deficiency of *kctd10* was responsible for the phenotype of $34c^{-/-}$, we injected *kctd10* mRNA into one-cell stage zebrafish embryos derived from the in-cross of $34c^{+/-}$ and found that the ratio of the mutant embryos was significantly less than 25% ($P<0.01$ by the χ^2 test.) (Supplementary Fig. 3). The wild-type embryos injected with *kctd10* mRNA were indistinguishable from the wild-type embryos injected with phosphate-buffered saline (PBS). The injection of a morpholino (MO) against the translation of *kctd10* into wild-type embryos resulted in a phenotype that was indistinguishable from the *34c* mutant (Fig. 1h,i, Supplementary Movie 3).

More importantly, we targeted *kctd10* in zebrafish by TALEN (transcription activator-like effector nucleases) and obtained F_1 fish with an 8 bp-deletion in exon3 of *kctd10* at one allele ($kctd10^{+/TALEN}$). About one-fourth of the offspring derived from

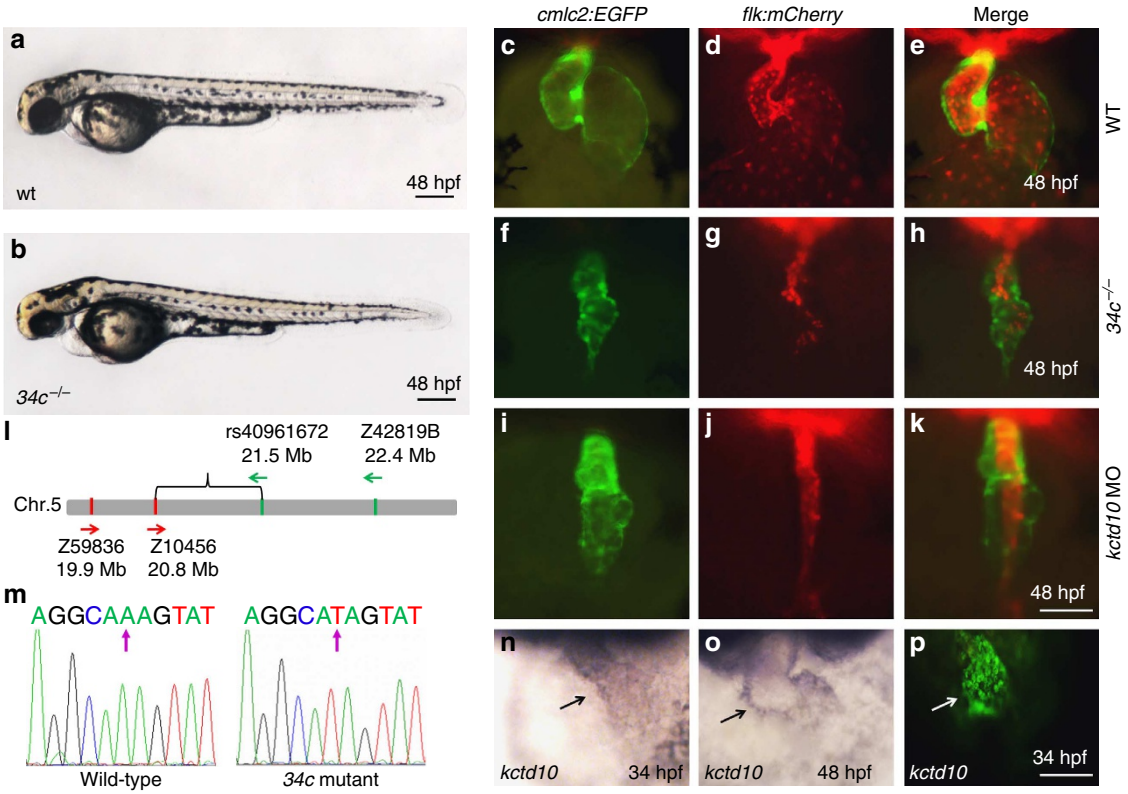

Figure 1 | *Kctd10* is responsible for the heart defect of the zebrafish mutant *34c*. (**a**,**b**) Bright-field micrographs of wild-type (wt) and *34c* mutant embryos at 48 hpf. The mutant exhibits certain pericardial oedema. Scale bars = 0.25 mm. (**c**–**k**) Fluorescence micrographs of the hearts of wild-type (**c**–**e**), *34c* mutant (**f**–**h**) and embryos injected with 4 ng MO against the translation of *kctd10* (**i**–**k**) at 48 hpf under the background of *Tg(cmlc2:EGFP)/Tg(flk:mCherry)* transgenic fish. Both the myocardium (green) and the endocardium (red) are substantially smaller in the mutant and the morphant, and no cavity is visible inside the heart lumen. Scale bar = 0.1 mm. (**l**) A genetic map of the *34c* mutant placed the affected gene between markers *Z10456* (Chr5: 20.84 Mb) and *rs40961672* (Chr5: 21.47 Mb) (Ensembl Zv9). (**m**) Sequencing result of *kctd10* cDNA revealed an A-to-T transversion at position 120 of exon 2. (**n**,**o**) *In situ* hybridization of *kctd10* in wild-type embryos. *Kctd10* was expressed in the heart (arrow) at 34 and 48 hpf. (**p**) Kctd10 protein detected by immunofluorescence. The heart tube is indicated by arrow. (**n**–**p**) Scale bar = 0.1 mm. (**c**–**k**,**n**–**p**) Ventral views with the anterior at the top.

the in-cross between *kctd10*$^{+/TALEN}$ showed the same phenotype as *34c* mutant. Complementation testing revealed that about one-fourth of the larvae (10/41 and 13/58 in two independent assays) from the cross between *kctd10*$^{+/TALEN}$ and *34c*$^{+/-}$ showed phenotypes very similar to *34c* mutants (Supplementary Fig. 4). These data demonstrate that the nonsense mutation of *kctd10* is responsible for the phenotype of the *34c* mutant.

Zebrafish Kctd10 protein is composed of 313 amino-acid residues and shares 94% identity with its orthologues in humans and mice (Supplementary Fig. 5). *In situ* hybridization revealed that *kctd10* mRNA was present in embryos at the one-cell stage, and its expression was ubiquitous until 24 hpf (Supplementary Fig. 6). At 34 hpf, *kctd10* was detected in the heart tube, the brain and the hatching gland (Fig. 1n; Supplementary Fig. 6). At 48 hpf, its expression was maintained in both the atrium and ventricle (Fig. 1o). Kctd10 protein was also present in the heart tube at 34 hpf (Fig. 1p).

***Kctd10* is required for AVC formation**. We investigated the expression of several common cardiac markers by *in situ* hybridization in *kctd10* mutants. At 18 hpf, when the myocardial precursors segregate into two populations adjacent to the midline, the expression of the heart tube marker *cmlc2* (cardiac myosin light chain 2) did not differ between the mutant and the wild-type (Supplementary Fig. 7a,b). These data suggest that the specification of the cardiac mesoderm is not affected in the mutant. The expression of *cmlc2* also showed no difference at 48 hpf (Supplementary Fig. 7c,d).

The ventricular marker *vmhc* (ventricular myosin heavy chain) and the atrial marker *amhc* (atrial myosin heavy chain, also known as *myh6*) were used to visualize the two chambers, respectively. At 48 hpf, *amhc* was detected in the atria of both the wild-type and mutant larvae (Supplementary Fig. 7e,f). *Vmhc* was detected in the ventricles of both the wild-type and mutant embryos (Supplementary Fig. 7g,h). The cardiac mesoderm marker *nkx2.5* was also examined and no difference was found between the *kctd10* mutants and their wild-type siblings (Supplementary Fig. 7i,j).

In contrast to the early genes necessary for cardiogenesis, the expression of the AV boundary marker genes, such as *bmp4*, *notch1b*, *tbx2b* and *has2*, was dramatically affected in the *kctd10* mutants. At 34 hpf, the expression patterns of *bmp4*, *notch1b* and *tbx2b* showed no difference between the mutants and the control embryos (Fig. 2a,b,e,f,i,j). In the heart of wild-type embryos at 48 hpf, *bmp4*, *notch1b* and *tbx2b* were expressed at the prospective AVC (Fig. 2c,g,k). However, *bmp4* and *tbx2b* expanded throughout the myocardium (Fig. 2d,l), and *notch1b* expanded over the entire endocardium in the mutant (Fig. 2h).

Has2 is essential for AVC formation[21–23]. Its expression was detected at the AVC region in the wild-type embryos (Fig. 2m,o); In the *kctd10* mutant embryos at 48 hpf, expression of *has2* expanded (Fig. 2p). More impressively, the ectopic expression of *has2* in the mutant embryos at 34 hpf was more remarkable than

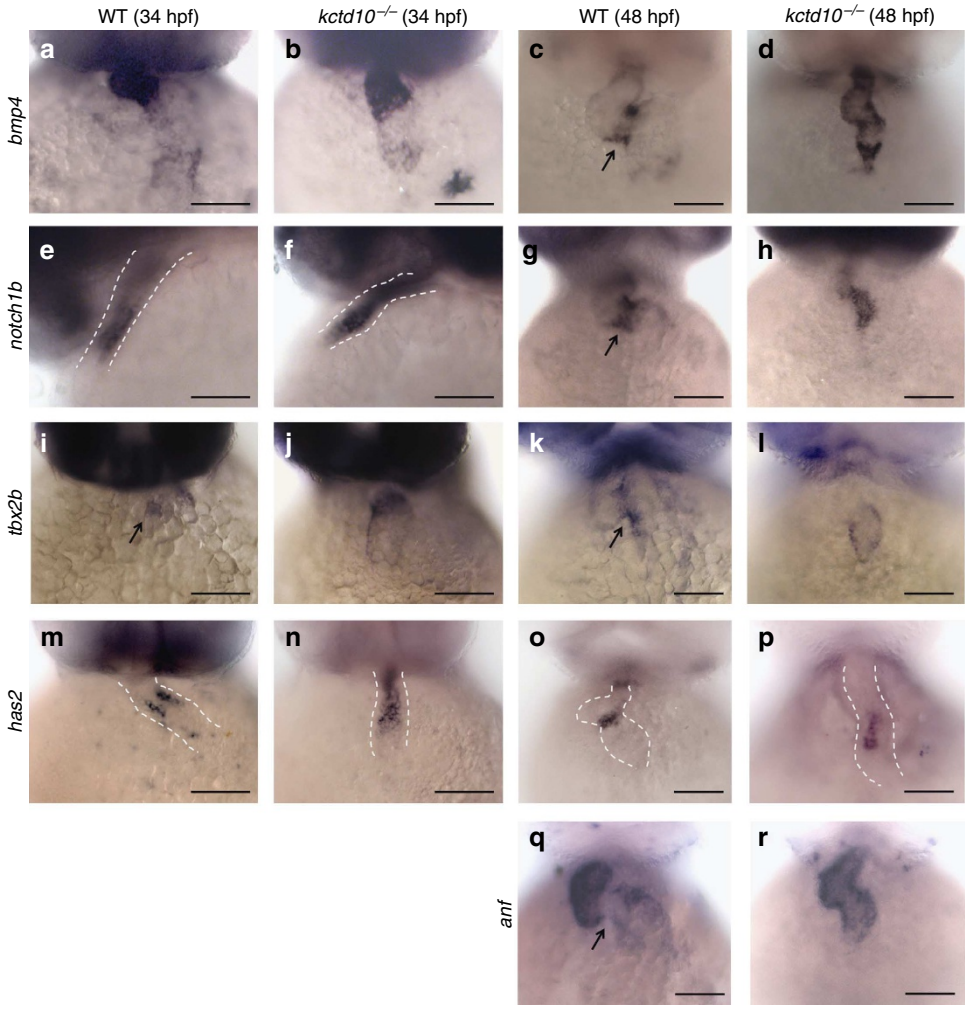

Figure 2 | The atrioventricular canal is malformed in the *kctd10* mutant. The expression of *bmp4*, *notch1b*, *tbx2b*, *has2* and *anf* in wild-type and *kctd10* mutant embryos at 34 and/or 48 hpf was shown by *in situ* hybridization. The expression patterns of *bmp4*, *notch1b* and *tbx2b* did not differ dramatically between the mutant and wild-type embryos at 34 hpf (**a**,**b**,**e**,**f**,**i**,**j**), but showed significant difference at 48 hpf (**c**,**d**,**g**,**h**,**k**,**l**). *Has2* were localized to a restricted region in wild-type embryos (**m**,**o**), while its expression expanded significantly in the mutant, especially at 34 hpf (**n**,**p**) The border of the heart is delineated with the dotted lines. The expression of *anf* was also upregulated and detected in the AVC in the mutant (**q**,**r**; the arrow in **q** indicates the AVC.) at 48 hpf. (**a**–**d**, **g**–**r**) Ventral views with the anterior at the top; (**e**,**f**) Lateral views with the anterior to the left. Scale bars = 0.1 mm.

in the mutants at 48 hpf (Fig. 2n). As mentioned above, the mutant embryos before 36 hpf was indistinguishable from their siblings. These results indicate that the ectopic expression of *has2* occurs before the emergence of the phenotype.

In the mutant, the myocardial chamber marker *anf*, also known as *nppa* (natriuretic peptide type A), was also upregulated and detected throughout the entire heart, including the AVC (Fig. 2q,r). The altered expression of these AVC marker genes indicates that the AVC in the *kctd10* mutant is malformed.

The mutations of the genes encoding the ion channel proteins usually result in heart malformations. To identify whether Kctd10 protein acts as a potassium channel, the K^+ flux around the surface of the heart was measured by the Scanning Ion-selective Electrode Technique (SIET). The K^+ showed net influx at the heart surface. No significant difference was detected between the *kctd10* mutants and their normal siblings (Supplementary Fig. 8).

Moreover, we have treated the *kctd10* mutant embryos with the drugs that could alter the heart contractility and/or heart rate, such as adrenaline, digilanid and atropine. Adrenaline increases the heart rate and elevates blood pressure. Digilanid increases myocardial contractility and blood pressure while reducing heart rate. Atropine is a muscarinic acetylcholinergic antagonist that increases firing of the sinoatrial node and conduction through the atrioventricular node of the heart. Both adrenaline and atropine increased the heart rates in both the wild-type and the mutant zebrafish embryos, while digilanid reduced the heart rate, as expected. However, none of the drugs were able to relieve the cardiac morphology of the mutant (Supplementary Fig. 9). These data demonstrate that the heart defects of kctd10 mutant are unlikely due to the physical forces.

Knockdown of *has2* alleviates the phenotype in the mutant. Has2 protein is the synthetase of hyaluronic acid, an extracellular glycosaminoglycan that is the major component of the cardiac jelly. Ectopic expression of *Has2* is reported to impair cardiac looping, results in lumen narrowing and increases the space between the endocardium and myocardium in the heart chambers[22]. This phenotype was also observed in the histological sections of *kctd10* mutants at 48 hpf (Fig. 3a,f). We stained hyaluronic acid by biotinylated hyaluronan-binding protein. The layer of hyaluronic acid in the cardiac jelly of the mutant was much thicker than that of the wild-type (Fig. 3b–j).

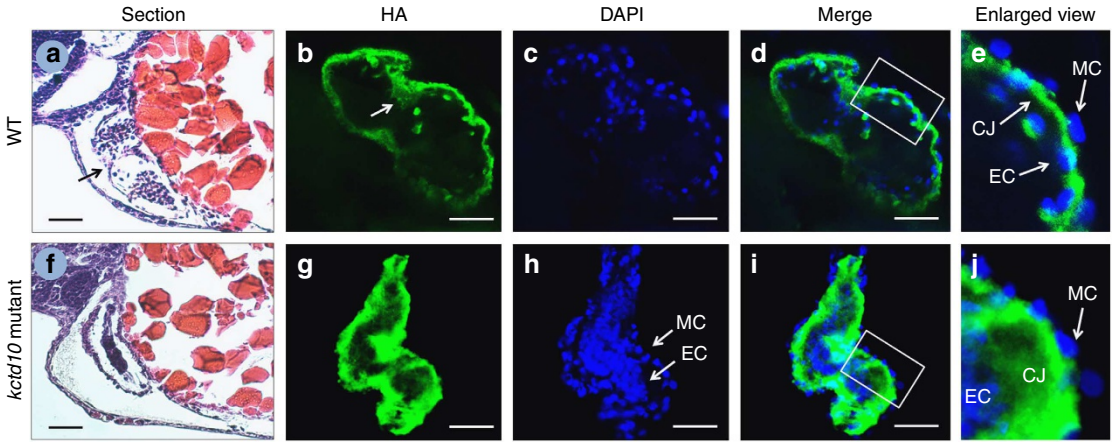

Figure 3 | The cardiac jelly in the *34c* mutant becomes thicker. (**a**,**f**), Histological sections of hearts from wild-type and mutant embryos at 48 hpf, staining with H&E. The endocardium of the mutant was extremely shrunken and the space between the myocardium and endocardium was much wider than that of the wild-type. The AVC (**a**, arrow) disappeared in the mutant (**f**). (**b**–**j**) Hyaluronic acid staining (green) and nucleus staining (blue) of the hearts of wild-type (**b**–**e**) and *kctd10* mutant (**g**–**j**) embryos at 48 hpf. The arrow in **b** indicates the endocardial cushions at AVC, where more HA is localized. (**e**,**j**) enlarged views of the atrium wall (boxed in **d**,**i**). CJ, cardiac jelly; EC, endocardial cells nuclei; MC, myocardial cells nuclei. Scale bars = 0.05 mm.

Cardiac jelly is essential for cardiac development, including the AVC formation and heart looping[28–30]. To clarify whether the ectopic expression of *has2* was the cause of the heart defect in the *kctd10* mutant, the MO against *has2* was injected into the embryos derived from the in-cross of *Tg(cmlc2:EGFP)*$^{34c+/-}$ fish. At 48 hpf, only 10% (6/59) of the embryos injected with 6 ng per embryo of *has2* MO had the same phenotype as the *kctd10* mutant (Supplementary Table 1). The hearts of the majority of the embryos were not shrunken, but the AVC became wider than that of the wild-type as described before[23] (Fig. 4a,b). The heart of these morphants exhibited a sequential, coordinated beating of the atrium and ventricle (Supplementary Movie 4, genotyped as wild-type). Functional circulation was also observed. Eight out of 59 embryos seemed to have normal cardiac morphogenesis and circulation. These eight embryos were genotyped and five of them were *kctd10* mutants (Fig. 4e; Supplementary Movie 5).

We also coinjected *has2* MO and *kctd10* MO into the wild-type embryos. Compared with the embryos injected with only *kctd10* MO, neither the myocardium nor the endocardium of 90% (50/56) embryos injected with both MOs showed a substantial decrease in size. More importantly, the heart looping in >20% (12/56) of the double morphants was recovered completely (Supplementary Fig. 10), whereas in 60% (38/56) double morphants, the heart looping was partially recovered and showed more mature hearts than in the *kctd10* morphants. The heart of the majority of the double morphants exhibited a sequential, coordinated beating of the atrium and ventricle.

In summary, repressing the expression of *has2* in *kctd10* mutants/morphants resulted in the recovery of the heart defects. Considering that the ectopic expression of *has2* occurs before the emergence of the phenotype, these data demonstrate that the ectopic expression of *has2* is the major cause of heart malformations in the *kctd10* mutants.

Knockdown of *tbx5a* alleviates heart defects in *kctd10* mutant. We wanted to determine what causes the ectopic expression of *has2*. We noticed that the phenotype of *kctd10* mutant, including the shrunken heart, the slower heart rate and the smaller pectoral fin, was similar to the zebrafish mutant *heartstrings*[31]. Thus, the expression of *tbx5a* was examined by *in situ* hybridization. Unexpectedly, the expression pattern of *tbx5a* in the mutants revealed no marked differences from the wild-type embryos (Supplementary Fig. 11). Also unexpectedly, injection of *tbx5a* mRNA was not able to rescue the phenotype of the mutants.

Considering that *Tbx5* overexpression resulted in a similar phenotype to *Tbx5* deficiency[26], we injected the MO against *tbx5a* into the embryos derived from the in-cross of the *Tg(cmlc2:EGFP)*$^{34c+/-}$ zebrafish strain. When we injected 3 ng of *tbx5a* MO, 13 out of 60 embryos exhibited the *kctd10* mutant phenotype, but 6 out of the 13 embryos showed weakened circulation at 48 hpf. The expression of *has2* in these mutants was also mildly decreased, indicating partial rescue (Supplementary Tables 1,2; Supplementary Fig. 12c). When 5 ng of *tbx5a* MO was injected into each embryo, the observed number of embryos with the mutant phenotype at 48 hpf was far less than expected (8/66) (Supplementary Table 1). Nine injected embryos had normal cardiac morphogenesis. These embryos were genotyped and eight of them were *kctd10* mutants (Fig. 4f; Supplementary Movie 6). The expression pattern of *has2* was also rescued in the mutants with normal phenotype (Supplementary Fig. 12e). Functional circulation was observed in these embryos. The hearts of the majority of the embryos shrank slightly, but exhibited a sequential, coordinated beating (Fig. 4c; Supplementary Movie 7, genotyped as wild-type). In the embryos with slightly shrunken hearts (12 of these embryos were genotyped and one was mutant), the expression of *has2* was not detected (Supplementary Fig. 12d,f). We also injected 6 ng of *tbx5a* MO into the embryos of *kctd10* mutants, and obtained the similar results (Supplementary Table 1).

As mentioned above, the ectopic expression of *has2* is the major cause of heart malformations in the *kctd10* mutants. Now that knock down of *tbx5a* was able to rescue the heart malformations in *kctd10* mutants, *tbx5a* MO should also rescue the ectopic expression of *has2* in the mutants at 34 hpf. Thus, we examined the expression of *has2* in *kctd10* mutants injected with *tbx5a* MO at 34 hpf. With the injection of 3 ng of *tbx5a* MO, *has2* was decreased in 6 out of 15 mutants, indicating partial rescue (Fig. 4i; Supplementary Table 2). In the rest nine mutants, the expression of *has2* was similar to that in the mutant injected with PBS. When injected with 5 ng of *tbx5a* MO, the expression of *has2* was restricted at the AV junction in 5 out of 16 mutants at 34 hpf; in 3 out of the 16 mutants, *has2* disappeared (Fig. 4k,l; Supplementary Table 2). Thus, knockdown of *tbx5a* could rescue both the heart malformations and the ectopic expression of *has2* in *kctd10* mutants.

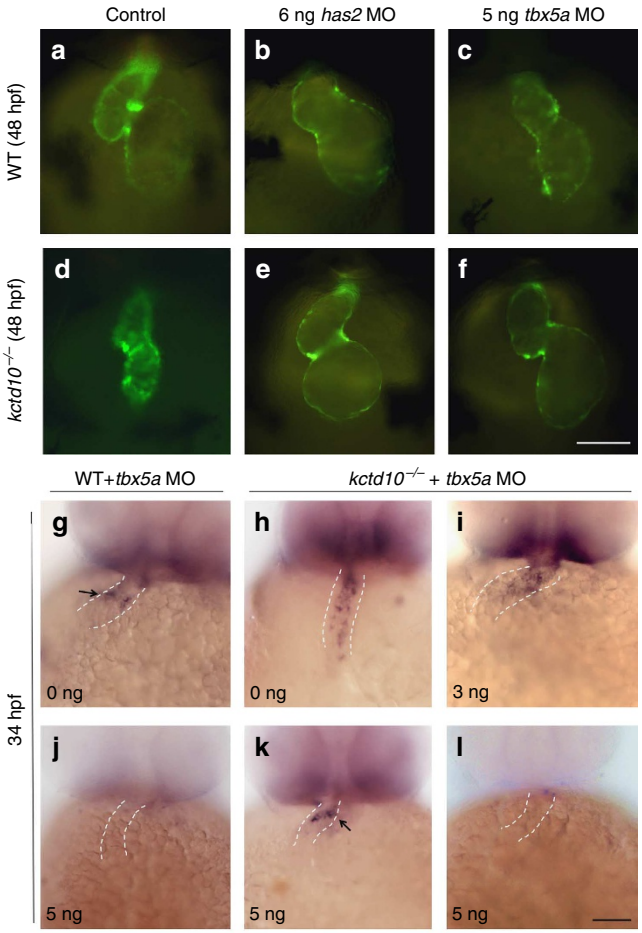

Figure 4 | The knockdown of *has2* or *tbx5a* alleviates the heart defect in *kctd10* mutants. (**a**–**f**) The MO against *has2* or *tbx5a* was injected into the embryos derived from the in-cross of *Tg(cmlc2:EGFP)*$^{+/34c}$ fish. The heart of the *kctd10* mutant (**d**) was markedly smaller than the wild-type embryos (**a**) at 48 hpf. The AVC of wt embryos injected with *has2* MO became wider (**b**), and the heart of wt embryos injected with *tbx5a* MO is slightly shrunken (**c**). (**e**,**f**) Some injected mutants have nearly normal cardiac morphogenesis. (**g**–**l**) *In situ* hybridization of *has2* in the mutants injected with *tbx5a* MO. *Has2* was expressed in the very restricted region of the endocardium in wild-type embryos (**g**, arrow), whereas it expanded throughout the endocardium of the heart tube in the *kctd10* mutants (**h**). When treated with 3 ng of *tbx5a* MO, the ectopic expression of *has2* decreased moderately in some mutants (**i**); in case of injection with 5 ng of *tbx5a* MO, *has2* was undetectable in wild-type embryo (**j**), but restricted at the AVC in 5/16 mutants (**k**, arrow); in 3/16 mutants, *has2* disappeared (**l**). All the embryos used here were genotyped. Ventral views with the anterior at the top. (**a**–**f**) Scale bar = 0.1 mm; (**g**–**l**) Scale bar = 0.1 mm.

The MO against *tbx5a* was also coinjected into wild-type embryos with the MO against *kctd10*. When 3 ng of *tbx5a* MO was injected into the embryos together with the *kctd10* MO, the expression of *has2* was recovered to normal in 8 out of 30 embryos. The ectopic expression of *has2* was moderately reduced in the other 22 embryos, indicating partial rescue (Supplementary Fig. 12h,i; Supplementary Table 2). When the dosage of 5 ng per embryo was used, the ectopic expression of *has2* was eliminated in 10 out of 24 samples, and *has2* expression disappeared in 14 out of 24 embryos (Supplementary Fig. 12k,l; Supplementary Table 2).

These data suggest that Tbx5a is hyperactivated in the *kctd10* mutants/morphants, although the expression of *tbx5a* does not alter much. It indicates that Kctd10 protein may play a role in repressing the transcriptional activity of Tbx5a. Considering that the dosage of Tbx5/5a is critical for cardiac morphogenesis and we could not control the dosage of *tbx5a* MO exactly, the knockdown of *tbx5a* did not rescue the cardiac malformations in all mutants/morphants.

Kctd10 directly binds to Tbx5/5a to repress its activity. To confirm that Kctd10 protein moderated the transcriptional activity of Tbx5, the reporter construct of *G5E1b-luciferase* and the expression vector *Gal4-Tbx5(266–518)* were used for reporter assay. *G5E1b-luciferase* contains five Gal4-binding elememts[32] and *Gal4-Tbx5(266-518)* contains the coding sequences of the Gal4 DNA-binding domain fused to Tbx5 transactivating domain in-frame[33]. The transactivating domain of Tbx5 dramatically stimulated the expression of the *Luciferase* gene (>600-fold). This strong activation was significantly suppressed by the expression of *Kctd10* in a dose-dependent manner (Fig. 5a). In contrast, Kctd10 had no effect on the activity of *G5E1b-luciferase* induced by *Gal4-VP16* (Fig. 5a).

We also examined whether Kctd10 could regulate the expression of a Tbx5 target gene. Luciferase reporter assays were performed with the constructs of *Anf(−0.7k)-Luc*, where *Luciferase* is driven by the regulatory region of mouse *Anf*[2,33]. The results showed that the activation of *Anf(−0.7k)-Luc* mediated by Tbx5 was markedly suppressed by Kctd10 in a dose-dependent manner (Fig. 5b). Kctd10 had no effect on the transactivation of *Anf* mediated by Gata4 alone (Fig. 5b).

Co-transfection of *Kctd10* also repressed the Tbx5-Gata4-mediated activation of the *Tbx2(−5.6/+0.316)-Luc* in a dose-dependent manner, whereas Kctd10 had no significant effect on either Bmp/Smad-mediated transactivation or TBX20-mediated suppression of *Tbx2* (Supplementary Fig. 13a–c). The expressions of Tbx5a target genes, including *amhc* (*myh6*), *tbx2b* and *anf*, were also examined by real-time reverse transcriptase–PCR or deep sequencing. The results showed that all these genes were upregulated in the *kctd10* mutant (Supplementary Fig. 13d,e; Supplementary Data 1). Thus, Kctd10 suppresses Tbx5a activity *in vivo*.

How does Kctd10 protein moderate the transcriptional activity of Tbx5? We performed co-immunoprecipitation (Co-IP) experiments to investigate their association. The precipitation of Flag-Kctd10 protein was able to pull down Tbx5a from the cell lysate, and the precipitation of HA-Tbx5a was able to pull down Kctd10 (Supplementary Figs. 13f and 15). HA-Tbx5a could also pull down endogenous KCTD10 (Supplementary Figs. 13g and 15).

The association between KCTD10 and TBX5 proteins was also confirmed *in vivo*. Immunoprecipitation of endogenous TBX5 with a polyclonal antibody against this protein specifically retrieved endogenous KCTD10 in HeLa cells, but not with the control immunoglobulin G of the rabbit. Consistently, anti-KCTD10 antibody was able to pull down TBX5 in the reciprocal co-IP assays (Fig. 5c; Supplementary Fig. 14). Thus, KCTD10 binding to TBX5 occurred in a cellular context. *In vitro* pull-down assays with glutathione S-transferase (GST)-Kctd10 fusion proteins was performed. These results show that Kctd10 protein directly binds to Tbx5a (Fig. 5d; Supplementary Fig. 14).

To determine the cellular localization of Kctd10 protein, the fusion constructs of *pEGFP-N1-KCTD10* and *pRK-TBX5-HA* were co-transfected into cells. The proteins were detected by green fluorescent protein (GFP)/immunofluorescence. The results showed the nuclear distribution of both KCTD10 and TBX5. KCTD10 protein colocalized with TBX5 in the nuclei (Fig. 5e).

These results reveal that Kctd10 protein directly binds to Tbx5/5a to moderate its transcriptional activity in the nucleus.

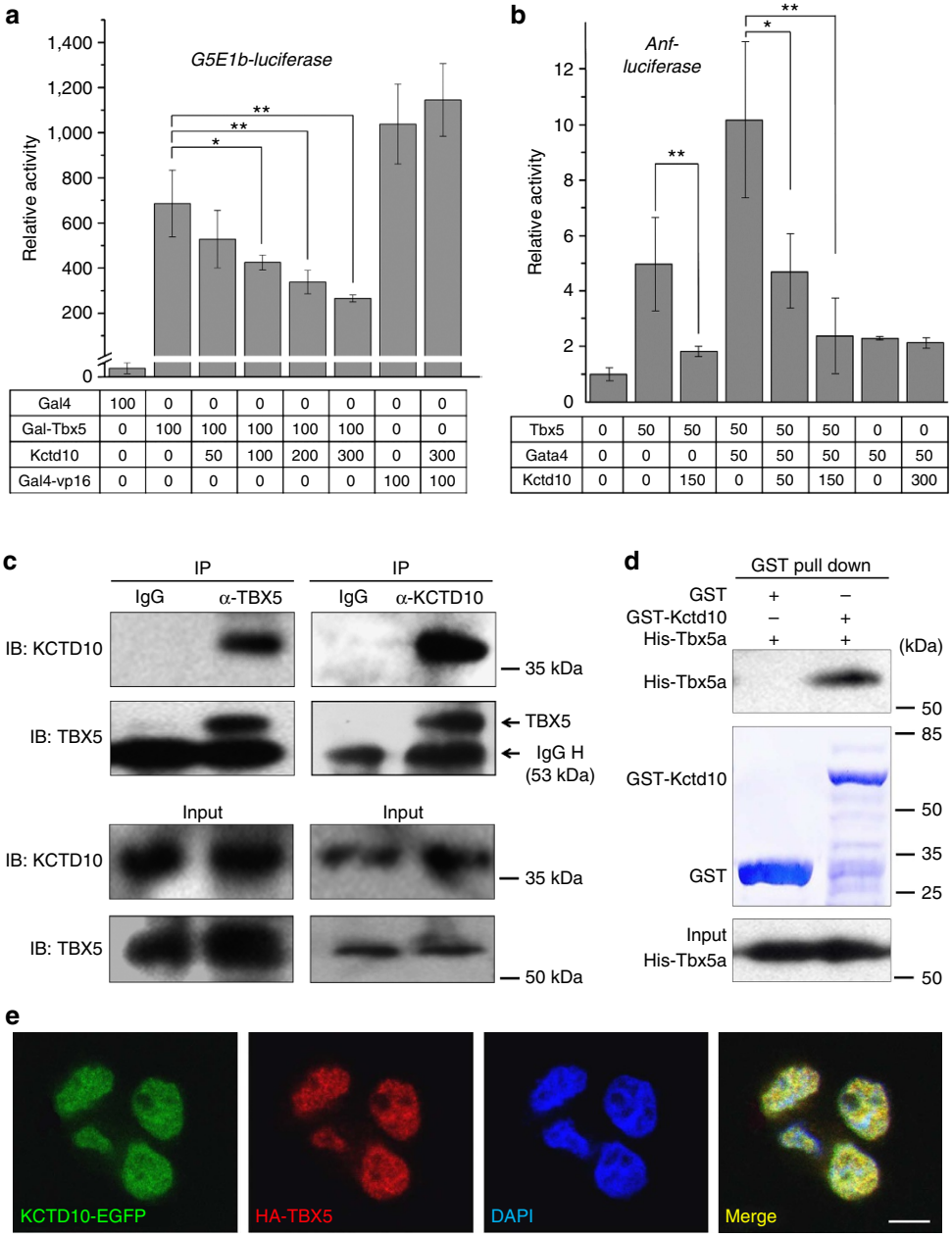

Figure 5 | Kctd10 directly binds to Tbx5/5a to moderate its transcriptional activity. (**a**,**b**) Luciferase reporter assays of the *G5E1b* and the 0.7-kb *Anf* promoter fragment. Numbers indicate the quantity (nanograms) of each corresponding plasmid. At least three independent experiments were performed for each assay, and each in quadruplicate (mean ± s.e.m.; $n = 4$). Asterisks represent the statistical significance as determined using a Student's *t*-test (*$P < 0.05$; **$P < 0.01$). (**c**) Co-IP of endogenous TBX5 and endogenous KCTD10 in HeLa cells. (**d**) Pull-down assay of His-tagged Tbx5a by GST fusion Kctd10 protein bound to GSH-agarose beads and subsequent detection by western with anti-His antibody. The expression of GST and GST fusion protein was stained by Coomassie brilliant blue. (**e**) Immunofluorescent detection of HA-Tbx5a and Kctd10-GFP in 293T cells. Nuclei are counterstained by DAPI. Scale bar = 10 μm.

Discussion

KCTD proteins comprise a large family and show high conservation across species. Few members of this family have been studied, aside from the following examples: KCTD5 mediates protein degradation in the proteasome[34]; KCTD 8, 12 and 16 regulate the function of $GABA_B$[35]; KCTD15 suppresses canonical Wnt signalling through an unidentified mechanism[36]; and KCTD10 interacts with proliferating cell nuclear antigen and DNA polymerase δ to regulate cell proliferation[37,38]. Recently, KCTD13 has been shown to relate to the copy number variant of 16p11.2 (ref. 39). Therefore, the functions of the KCTD proteins are quite diverse. However, *KCTD* genes have not been targeted in any model animals, and thus their roles in development are unknown. Here we demonstrate that Kctd10 plays a key role in cardiac morphogenesis via repressing the transcriptional activity of Tbx5.

Tbx5 is a dose-sensitive transcription factor, so it needs to be tightly regulated. Very little is known about its regulation. JAK-STAT3 signalling is important for the expression of Tbx5, whereas PDZ and LIM domain protein 7 (Pdlim7) inactivates Tbx5 by tethering it in the cytoplasm[40]. Tbx20 also antagonizes Tbx5 function by repressing its expression[32].

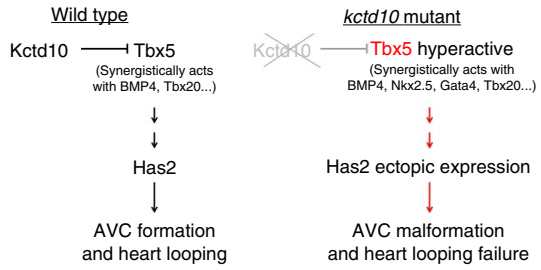

Figure 6 | A model of Kctd10 function in cardiogenesis. In wild-type zebrafish embryos, the transcriptional activity of Tbx5 is moderated by Kctd10, and Tbx5 synergistically acts with other factors to restrict *has2* at the prospective AVC region. When Kctd10 is deficient, Tbx5 is hyperactive to result in the ectopic expression of *has2*. Excess hyaluronic acid is deposited between myocardium and endocardium throughout the heart tube to lead to the malformations of AVC and heart looping failure.

Our data reveal a new mechanism of the regulation of Tbx5. Kctd10 physically binds to Tbx5 to modify the activity of the transactivating domain rather than control *Tbx5* expression. Since Kctd10 and Tbx5 are colocalized in the nucleus, Kctd10 might be involved in the protein complex formed by Tbx5 and other factors, such as Tbx20, Nkx2.5 and Gata4. This regulation of Tbx5 is critical to restrict the expression of *has2*, one of the critical genes for the formation of AVC, in the specific region of the heart tube. The ectopic expression of *has2* causes heart malfornations[8,22], that are very similar to the phenotype of *kctd10* mutant. We confirmed that the heart defect in *kctd10* mutant is due to the ectopic expression of *has2*.

On the basis of our findings and others' previous work, we present a model to delineate the role of Kctd10 in heart morphogenesis (Fig. 6). In the developing heart of the wild-type zebrafish embryo, the transcriptional activity of Tbx5 is moderated by Kctd10 to maintain its activity at a proper level. Tbx5 synergistically acts with other factors, such as BMP4, Nkx2.5, Gata4 and Tbx20, to restrict the expression of *has2* at the AV boundary of the heart tube. Has2 catalyses the synthesis of hyaluronic acid, the major component of cardiac jelly, thus the cardiac jelly swells at the AVC. Has2 also plays a pivotal role in the epithelium-to-mesenchyme transformation of the endocardium at the AV boundary, which gives rise to the endocardial cushions and valves[22,23,27]. In the forming heart of the *kctd10* mutant, Tbx5 is hyperactive due to the absence of functional Kctd10. As a result, *has2* is no longer restricted to the AV boundary, but expands throughout the heart tube. The ectopic expression of *has2* results in excess hyaluronic acid between the myocardium and endocardium, causing the cardiac jelly to swell throughout the entire heart tube. The excessive cardiac jelly affects the cross-talk between the myocardium and endocardium to cause the heart malformations[23,27,41].

In summary, we have isolated a zebrafish mutant strain with heart malformations and found that *kctd10* is the affected gene. The Kctd10 protein plays a key role in restricting the expression of *has2* to the AVC by directly binding to Tbx5 to moderate its transcriptional activity. Since Kctd10 and Tbx5 are colocalized in the nucleus, Kctd10 is likely to act as a co-repressor of Tbx5 epigenetically. Therefore, Kctd10 is an important factor for cardiac development, which may be considered as a new candidate for the genetic screening and identification of congenital heart diseases in the future.

Methods

Zebrafish maintenance. All the experimental procedures followed the rules of the Committee on Animal Care of Beijing, China (5 June 2008). All animal experiments were approved by Institutional Animal Care and Use Committee (IACUC) of Peking University. The reference from IACUC of Peking University is LSC-ZhangB-1.

Zebrafish were raised and maintained at 28 °C in a circulating system that continuously filters, UV treats and aerates the circulating water. The in-tank breeding was used to obtain the embryos. The embryos were collected and raised in the incubator at 28 °C. The microinjection was performed at the one-cell stage. The larvae were anesthetized with 0.16 mg ml^{-1} Tricaine (MS-222, ethyl-3-amino-benzoate methanesulfonate salt, Sigma-Aldrich Inc.) before use[42].

Expression vectors and reporter plasmids. The *pAC-CMV-Tbx5*, *Gal4-Tbx5-(266–518)*, *pAC-CMV-Tbx20*, *pMT2-GATA4*, *Gal4-VP16* expression plasmids and the *G5E1b-luciferase* reporter plasmids were kindly provided by Dr Katherine E. Yutzey[33]. The reporter plasmid of *Tbx2(5.6/−0.316)-Luciferase* was kindly provided by Dr A. Kispert[2].

Flag-kctd10 was generated by amplifying the zebrafish *kctd10* sequence using the primer pair 5′-ATTTGCGGCCGCTATGGAAGAGATGTCAG-3′ and 5′-GAA GATCTGCGTAACTGAAGCG CTGGT-3′. The resulting PCR fragment was ligated into the NotI and BamHI sites of the *p3 × FLAG-CMV-7.1* (Sigma) plasmid. The mouse *Kctd10* expression vector that was used in reporter assay was constructed by amplifying the mouse *Kctd10* sequence using primers 5′-CCAAG CTTTTCATGGAAGAGATGTCA-3′ and 5′-AAGATATCACTGGTGGAGGTG GG CCC-3′. The resulting PCR fragment was ligated into the HindIII and EcoRV sites of the *p3 × FLAG-CMV-7.1*. Human *KCTD10* was amplified with primers 5′-GAAGATCTCCTG CGTCCTCCGACTTTT-3′ and 5′-AACTGCAGCTGGT GGAGGT GGGCCCG-3′ and ligated into the BglII and PstI sites of *pEGFP-N1* (Clontech). To generate the *Anf (−0.7)-luciferase* reporter, the 0.7-kb upstream fragment of the mouse *Anf* gene was amplified by PCR using the primers 5′-AAG GTACCCATCCTGTTGGCACCTTG-3′ and 5′-CACTCGAGTTTGCTGTCTC TGCCCAC TC-3′, the fragment was then ligated into the XhoI and KpnI sites of *pGL3* vector (Promega). *HA-tbx5a* was generated by amplifying the zebrafish *tbx5a* sequence using the primers 5′-ATTTGCGGCCGCTATGGCGGACAGTGAAG-3′ and 5′-GATCGTCGACCTGCATGTTAGC TGGC-3′; mouse *Tbx5* which was used in reporter assay was amplified with 5′-ATGCGGCCG CGATACAGATGA GGGCTT-3′ and 5′-GCGTCGACAGGTCAGCCTTTAGCTATTC-3′; human: 5′-ATGCGGCCGCAGTTGGAGAGCAGAACCTT-3′ and 5′-GCGTCGACGTC TGTTGTGAAGC AGGCCTCA-3′. The resulting PCR fragments were ligated into the NotI and SalI sites of *pCMV-3 × HA Hygro* plasmid.

Positional cloning. We mapped the *34c* locus to linkage group 5 using a panel of 119 microsatellite markers selected from the publicly available zebrafish genetic map[43]. For fine-mapping, 684 mutant embryos were screened with simple sequence length polymorphisms and restriction fragment length polymorphism markers. The complementary DNA of the 10 genes in the critical interval was then sequenced and analysed.

Morpholino and mRNA injections. Morpholino antisense oligonucleotides were dissolved in water at a concentration of 1 mM. The amount of the MOs used for injection was as follows: *kctd10* MO, 4 ng per embryo; *tbx5a* MO, 5 ng per embryo; *has2* MO, 6 ng per embryo. For each embryo, 1 nl of MO solution was injected into the cytoplasm. The sequence of MOs are: *kctd10* ATG MO, 5′-TCT CTTCCATAGAAATTCCCCGATT-3′; *has2* MO, 5′-AGCAGCTCTTTGGAGA TGTCCCGTT-3′; *tbx5* MO, 5′- GAAA GGTGTCTTCACTGTCCGCCAT-3′ (Gene Tools)[44,45]. Full-length capped zebrafish *kctd10* mRNA was prepared using the SP6 mMessage mMachine kit (Ambion).

For rescue assay, the MO against *tbx5* or *has2* was injected into the cytoplasm of one-cell stage embryos derived from the in-cross of *Tg(cmlc2:EGFP)*$^{34c+/-}$. The samples used for heart visualization or *in situ* hybridization were all genotyped for the status of *kctd10* gene after observation.

***In situ* hybridization.** Whole-mount *in situ* hybridization using digoxigenin-labelled antisense RNA probes were performed according to the standard protocols[46]. Briefly, the embryos were fixed in 4% paraformaldehyde at 4 °C overnight, and then dehydrated with alcohol. After the treatment of proteinase K, the embryos were put into the pre-hybridization buffers and incubated for 2 ~ 5 h at 65 °C. Then the probe was added into the buffer and incubated at 65 °C overnight. After washing, the samples were incubated with phosphatase-conjugated antibody against digoxigenin at 4 °C overnight. The next day, the samples were stained with NBT (Nitro Blue Tetrazolium)-BCIP (X- phosphate) (C3206, Berotime). Stained embryos were transferred into 3% methylcellulose (Sigma) and photographed under Imager A1 microscope (Zeiss) equipped with a digital camera (AxioCam MRc 5, Zeiss).

The isolation of zebrafish heart and deep sequencing. The hearts were isolated from the wild-type fish and the *kctd10* mutant fish under the background of Tg (cmlc2:EGFP) as described previously[47]. Briefly, embryos of Tg (*cmlc2:GFP*) suspended in the ice-cold L-15 Medium (Invitrogen, Carlsbad, CA, USA) containing 10% fetal bovine serum (Hyclone, Logan, UT, USA) and Tricaine were

sucked into a 1 ml needle-free syringe (Shanghai Zhiyu medical material Co Ltd). The needle was added to the syringe and the medium containing the embryos in the syringe was immediately expelled into a new dish containing the same medium. The intact GFP$^+$ hearts were identified and picked up with a p20 micropipet under fluorescent light.

Total RNAs from wild-type and *kctd10* mutant fish hearts were isolated with RNeasy Mini Kit (Qiagen), purified with RNeasy columns (QIAGEN). Next-generation sequencing libraries were prepared with the Illumina TruSeq preparation kit (Illumina) according to the manufacturer's protocol and sequenced by the Illumina Hiseq 2000 platform. Around 200 million 50-bp single-end reads were obtained per sample. Reads were aligned to zebrafish genome Zv9 using tophat[48], with up to two mismatches allowed. Differential expression analysis was performed using DESeq[49].

TALEN construction and microinjection. The pair of TALENs recognizing the exon 3 of zebrafish *kctd10* was designed using TALE-NT[50] and the TAL effector repeats were constructed by 'unit assembly'[51]. TALEN mRNA was synthesized by *in vitro* transcription using SP6 mMESSAGE mMACHINE Kit (Ambion). The fragments containing the TALEN target site was amplified by PCR and digested with HpaII to examine the efficiency of TALENs and to determine the phenotype in F_1. The primers used are: Forward 5′-TGTGTGCTTCTGCAACATCCT-3′; Reverse 5′-GACACTCATCTACCAGGCCC-3′.

Transfections of culture cells and reporter assays. 293T cells (American Type Culture Collection, ATCC) were cultured in DMEM (Dulbecco's modified Eagle's medium) containing 10% fetal bovine serum (Hyclone) and 100 units ml^{-1} of penicillin/streptomycin (Invitrogen). Cells were plated in 24-well plates, then co-transfected with 300–500 ng of each expression vector and 100 ng of the reporter plasmid using Lipofectamine 2000 (Invitrogen). The amount of total DNA was equalized by the addition of empty expression vectors. Cells were harvested 24 h after transfection. Luciferase activity was measured using the Dual-Luciferase Reporter Assay System (Promega) according to the manufacturer's instructions. At least three independent experiments were performed for each assay and each experiment was performed in quadruplicate. Statistical significance was determined using a Student's *t*-test.

Co-immunoprecipitation. The whole-cell lysates of HeLa cells (ATCC) were incubated with 2 μg anti-TBX5 (bs-2354R, Bioss Inc.), 2 μg anti-KCTD10 (LS-C30750, LifeSpan Bioscience) for 12 h at 4 °C with end-over-end rotation, respectively. Protein A/G agarose beads were added and the reaction mixtures were further mixed for 3 h at 4 °C. After washed with lysis buffer for five times, proteins were extracted from the agarose beads by boiling in 2 × SDS gel-loading buffer and resolved on SDS-polyacrylamide gels. Western blotting was performed with anti-TBX5 (BIOSS) and anti-KCTD10 (LifeSpan Bioscience), respectively.

293T cells cultured in 10 cm dishes were transfected with *HA-tbx5/5a* and *Flag-kctd10* expression constructs. After 36 h, cells were washed once with PBS and harvested. Total cell extracts were prepared in cell lysis buffer (20 mM Tris–HCl, pH 7.5, 150 mM NaCl, 10 mM NaF, 20 mM β-glycerophosphate, 1 mM sodium orthovanadate, 1 mM PMSF, 10 μg ml^{-1} leupeptin, 2 μg ml^{-1}aprotinin, 1% Triton X-100 and 1 mM EDTA). Cell lysate were mixed with HA or Flag antibodies at 4 °C for 4 h. Then lysates were incubated with Protein A and Protein G agarose (GE Healthcare) for an additional 1 h. Immune complexes were washed five times with lysis buffer. The immunocomplexes were resolved by SDS–polyacrylamide gel electrophoresis (PAGE), and western blotting was performed with the following antibodies: anti-Flag M2 (Sigma); anti-HA (Y-11) (Santa Cruz Biotechnology); anti-KCTD10 (LSBio); horseradish peroxidase-conjugated goat anti-mouse, anti-rabbit antibody (Thermo).

A431 cells (ATCC) were transfected with HA-TBX5 expression construct. After 36 h, cells were washed once with PBS and harvested. Total cell extracts were prepared in cell lysis buffer (20 mM Tris–HCl (pH 7.5), 150 mM NaCl, 10 mM NaF, 20 mM β-glycerophosphate, 1 mM sodium orthovanadate, 1 mM PMSF, 10 μg ml^{-1} leupeptin, 2 μg ml^{-1} aprotinin, 1% Triton X-100 and 1 mM EDTA). Cell lysates were mixed with HA antibodies at 4 °C for 4 h. Then lysates were incubated with Protein A and Protein G agarose (GE Healthcare) for an additional 1 h. Immune complexes were washed five times with lysis buffer. Immunocomplexes were resolved by SDS–PAGE, and western blotting was performed with anti-HA antibody (Y-11) (Santa Cruz Biotechnology).

GST Pull-down assays. *Escherichia coli* BL21 harboring expression vectors for *GST-kctd10*, *His-tbx5a*, or GST alone, *His-tbx5a* were grown to $A_{600} = 0.6 \sim 0.8$ and induced with isopropyl β-D-1-thiogalactopyranoside for 6 h. Purified His-Tbx5a from *E. coli* BL21 was incubated with GST or GST-Kctd10 bound to glutathione–Sepharose beads. The beads were collected by centrifugation and washed five times with PBS. Proteins retained on the beads were then blotted with the anti-His antibody (1:500; Santa Cruz Biotechnology).

Immunofluorescence staining. 293T cells grown on coverslips in six-well plates were transfected with *KCTD10-EGFP* and *HA-TBX5* expression constructs. After 36 h, cells were washed once with PBS and fixed with 4% formaldehyde in PBS for 10 min at room temperature. Cells were then rinsed with PBS, incubated with blocking solution (0.2% Triton X-100, 3% bovine serum albumin and 1 mM NaN_3 in PBS) for 30 min at 37 °C and incubated with 2 μg ml^{-1} HA antibody in blocking solution for 4 h. For immunostaining of Kctd10 in zebrafish embryos, the sample was fixed with 4% formaldehyde in PBS overnight at 4 °C, then treated with blocking solution containing 0.2% Triton X-100 (v/v) for 2 h and incubated with the antibody against KCTD10 (1:300; LSBio, LS-C30750) overnight at 4 °C. After washed four times with PBS, the specimen was incubated with 20 μg ml^{-1} of goat anti-rabbit antibody (Alexa Fluor 594, Invitrogen) in blocking solution for 1 h, and then washed four times with PBS. The cells were incubated with DAPI (1 μg ml^{-1}) in washing solution for 2 min and mounted in 90% glycerol and sealed with nail polish.

Hyaluronan staining. As described above, the, the hearts were isolated from the wild-type fish and the *kctd10* mutant fish under the background of *Tg*(*cmlc2:EGFP*). The hyaluronan was stained as described[52]. Briefly, the tissue was fixed in acid-formalin-ethanol fixative (3.7% formaldehyde-PBS, 70% ethanol and 5% glacial acetic acid, all v/v) for 30 min, blocked in 1% bovine serum albumin containing 0.2% Triton X-100 (v/v) for 30 min at room temperature, then incubated with biotinylated hyaluronan-binding protein (HABP) (EMD/Millipore/Calbiochem #385911, diluted to 5 mg ml^{-1}) at 4 °C overnight. After four washes with PBS, the samples were treated with Fluorescent Streptavidin Construct (Alexa Fluor 488 conjugate, Molecular Probes, S-11223, diluted to 2 μg ml^{-1}) at room temperature for 2 h. The specimen was incubated with DAPI (1 μg ml^{-1}) in washing solution for 20 min and washed the samples for four times.

All the fluorescence samples were visualized under a fluorescence microscope (Axioimager Z1; Zeiss, Germany) or confocal laser scanning microscopes (LSM-710NLD & Duo Scan).

Pharmacology and quantification of heart rate. Adrenaline, digilanid and atropine were provided by Peking University Hospital. The embryos of 24 hpf derived from the incross of *kctd10*$^{+/-}$ zebrafish were treated with adrenaline (250 μM), atropine (100 μM) and digilanid (10 μM), respectively[53–55]. After incubating at 28 °C for 24 h, the larvae were anesthetized with MS-222 (ethyl-3-aminobenzoate methanesulfonate salt, Sigma-Aldrich Inc.) at 28 °C. After 5 min, the images of the larvae were captured by a digital video camera attached to the microscope (Camtasia Studio) and the heart rate was calculated from the captured images[53,56].

Scanning Ion-selective Electrode Technique. SIET[57] was used to measure extracellular K^+ flux at the surface of zebrafish larvae heart with a potassium-specific electrode. The assay was performed at room temperature in a small petridish filled with 1 ml PBS. The larvae hearts labelled with GFP were isolated as described above. For each sample, three different areas of the heart surface were measured.

References

1. Glickman, N. S. & Yelon, D. Cardiac development in zebrafish: coordination of form and function. *Semin. Cell Dev. Biol.* **13,** 507–513 (2002).
2. Singh, R. *et al.* Tbx20 interacts with smads to confine *Tbx2* expression to the atrioventricular canal. *Circ. Res.* **105,** 442–452 (2009).
3. Christoffels, V. M. & Burch, J. B. E. Moorman AFM. Architectural plan for the heart: early patterning and delineation of the chambers and the nodes. *Trends Cardiovasc. Med.* **14,** 301–307 (2004).
4. Bruneau, B. G. Transcriptional regulation of vertebrate cardiac morphogenesis. *Circ. Res.* **90,** 509–519 (2002).
5. Harvey, R. P. Patterning the vertebrate heart. *Nat. Rev. Genet.* **3,** 544–556 (2002).
6. Peterkin, T., Gibson, A., Loose, M. & Patient, R. The roles of GATA-4, -5 and -6 in vertebrate heart development. *Semin. Cell Dev. Biol.* **16,** 83–94 (2005).
7. Vermot, J. *et al.* Reversing blood flows act through *klf2a* to ensure normal valvulogenesis in the developing heart. *PLoS Biol.* **7,** e1000246 (2009).
8. Chi, N. C. *et al.* Foxn4 directly regulates *tbx2b* expression and atrioventricular canal formation. *Genes Dev.* **22,** 734–739 (2008).
9. Merscher, S. *et al.* Tbx1 is responsible for cardiovascular defects in velo-cardio-facial/ diGeorge syndrome. *Cell* **104,** 619–629 (2001).
10. Li, Q. Y. *et al.* Holt-Oram syndrome is caused by mutations in *TBX5*, a member of the *Brachyury(T)* gene family. *Nat. Genet.* **15,** 21–29 (1997).
11. Bruneau, B. *et al.* A murine model of Holt-Oram syndrome defines roles of the T-box transcription factor Tbx5 in cardiogenesis and disease. *Cell* **106,** 709–721 (2001).
12. Christoffels, V. M. *et al.* T-Box transcription factor Tbx2 represses differentiation and formation of the cardiac chambers. *Dev. Dyn.* **229,** 763–770 (2004).
13. Rochais, F., Mesbah, K. & Kelly, R. G. Signaling pathways controlling second heart field development. *Circ. Res.* **104,** 933–942 (2009).

14. Greulich, F., Rudat, C. & Kispert, A. Mechanisms of T-box gene function in the developing heart. *Cardiovasc. Res.* **91,** 212–222 (2011).
15. Habets, P. E. *et al.* Cooperative action of Tbx2 and Nkx2.5 inhibits ANF expression in the atrioventricular canal: implications for cardiac chamber formation. *Genes Dev.* **16,** 1234–1246 (2002).
16. Hoogaars, W. M. *et al.* The transcriptional repressor Tbx3 delineates the developing central conduction system of the heart. *Cardiovasc. Res.* **62,** 489–499 (2004).
17. Jerome, L. A. & Papaioannou, V. E. DiGeorge syndrome phenotype in mice mutant for the T-box gene, Tbx1. *Nat. Genet.* **27,** 286–291 (2001).
18. Lindsay, E. A. *et al.* Tbx1 haploinsufficiency in the DiGeorge syndrome region causes aortic arch defects in mice. *Nature* **410,** 97–101 (2001).
19. Olson, E. N. Gene regulatory networks in the evolution and development of the heart. *Science* **313,** 1922–1927 (2006).
20. Camarata, T. *et al.* Pdlim7 (LMP4) regulation of Tbx5 specifies zebrafish heart atrio-ventricular boundary and valve formation. *Dev. Biol.* **337,** 233–245 (2010).
21. Shirai, M., Imanaka-Yoshida, K., Schneider, M. D., Schwartz, R. J. & Morisaki, T. T-box 2, a mediator of Bmp-Smad signaling, induced hyaluronan synthase 2 and Tgfbeta2 expression and endocardial cushion formation. *Proc. Natl Acad. Sci. USA* **106,** 18604–18609 (2009).
22. Lagendijk, A. K., Goumans, M. J., Burkhard, S. B. & Bakkers, J. MicroRNA-23 restricts cardiac valve formation by inhibiting *Has2* and extracellular hyaluronic acid production. *Circ. Res.* **109,** 649–657 (2011).
23. Camenisch, T. D. *et al.* Disruption of hyaluronan synthase-2 abrogates normal cardiac morphogenesis and hyaluronan-mediated transformation of epithelium to mesenchyme. *J. Clin. Invest* **106,** 349–360 (2000).
24. Naiche, L. A., Harrelson, Z., Kelly, R. G. & Papaioannou, V. E. T-Box genes in vertebrate development. *Annu. Rev. Genet.* **39,** 219–239 (2005).
25. Hatcher, C. J. & Basson, C. T. Getting the T-box dose right. *Nat. Med.* **7,** 1185–1186 (2001).
26. McDermott, D. A. *et al.* TBX5 genetic testing validates strict clinical criteria for Holt-Oram syndrome. *Pediatr. Res.* **58,** 981–986 (2005).
27. Patra, C. *et al.* Nephronectin regulates atrioventricular canal differentiation via Bmp4-Has2 signaling in zebrafish. *Development* **138,** 4499–4509 (2011).
28. Armstrong, E. J. & Bischoff, J. Heart valve development: endothelial cell signaling and differentiation. *Circ. Res.* **95,** 459–470 (2004).
29. Hsieh, P. C. H., Davis, M. E., Lisowski, L. K. & Lee, R. T. Endothelial-cardiomyocyte interactions in cardiac development and repair. *Annu. Rev. Physiol.* **68,** 51–66 (2006).
30. Holtzman, N. G., Schoenebeck, J. J., Tsai, H. J. & Yelon, D. Endocardium is necessary for cardiomyocyte movement during heart tube assembly. *Development* **134,** 2379–2386 (2007).
31. Garrity, D. M., Childs, S. & Fishman, M. C. The heartstrings mutation in zebrafish causes heart/fin Tbx5 deficiency syndrome. *Development* **129,** 4635–4645 (2002).
32. Huang, J., Weintraub, H. & Kedes, L. Intramolecular regulation of MyoD activation domain conformation and function. *Mol. Cell Biol.* **18,** 5478–5484 (1998).
33. Plageman, Jr. T. F. & Yutzey, K. E. Differential expression and function of Tbx5 and Tbx20 in cardiac development. *J. Biol. Chem.* **279,** 19026–19034 (2004).
34. Bayón, Y. *et al.* KCTD5, a putative substrate adaptor for cullin3 ubiquitin ligases. *FEBS J.* **275,** 3900–3910 (2008).
35. Schwenk, J. *et al.* Native GABAB receptors are heteromultimers with a family of auxiliary subunits. *Nature* **465,** 231–235 (2010).
36. Dutta, S. & Dawid, I. B. Kctd15 inhibits neural crest formation by attenuating Wnt/beta-catenin signaling output. *Development* **137,** 3013–3018 (2010).
37. Zhou, J. *et al.* A novel PDIP1-related protein, KCTD10, that interacts with proliferating cell nuclear antigen and DNA polymerase delta. *Biochim. Biophys. Acta.* **1729,** 200–203 (2005).
38. Wang, Y. *et al.* KCTD10 interacts with proliferating cell nuclear antigen and its down-regulation could inhibit cell proliferation. *J. Cell Biochem.* **106,** 409–413 (2009).
39. Golzio, C. *et al.* KCTD13 is amajor driver of mirrored of the 16p11.2 copy number variant. *Nature* **485,** 363–367 (2012).
40. Snyder, M., Huang, X. Y. & Zhang, J. J. Stat3 directly controls the expression of *Tbx5*, *Nkx2.5*, and *GATA4* and is essential for cardiomyocyte differentiation of P19CL6 cells. *J. Biol. Chem.* **285,** 23639–23646 (2010).
41. Smith, K. A. *et al.* Rotation and asymmetric development of the zebrafish heart requires directed migration of cardiac progenitor cells. *Dev. Cell* **14,** 287–297 (2008).
42. Westerfield, M. *The Zebrafish Book: a Guide for the Laboratory Use of Zebrafish (Brachydanio rerio)* (University of Oregon Press, 1993).
43. Knapik, E. W. *et al.* A microsatellite genetic linkage map for zebrafish (*Danio rerio*). *Nat. Genet.* **18,** 338–343 (1998).
44. Bakkers, J. *et al.* Has2 is required upstream of Rac1 to govern dorsal migration of lateral cells during zebrafish gastrulation. *Development* **131,** 525–537 (2004).
45. Ahn, D.-G., Kourakis, M. J., Rohde, L. A., Silver, L. M. & Ho, R. K. T-box gene *tbx5* is essential for formation of the pectoral limb bud. *Nature* **417,** 754–758 (2002).
46. Alexander, J., Stainier, D. Y. & Yelon, D. Screening mosaic F1 females for mutations affecting zebrafish heart induction and patterning. *Dev. Genet.* **22,** 288–299 (1998).
47. Burns, C. G. & MacRae, C. A. Purification of hearts from zebrafish embryos. *Biotechniques* **40,** 278–281 (2006).
48. Trapnell, C., Pachter, L. & Salzberg, S. L. TopHat: discovering splice junctions with RNA-Seq. *Bioinformatics* **25,** 1105–1111 (2009).
49. Anders, S. & Huber, W. Differential expression analysis for sequence count data. *Genome Biol.* **11,** R106 (2010).
50. Doyle, E. L. *et al.* TAL Effector-Nucleotide Targeter (TALE-NT) 2.0: tools for TAL effector design and target prediction. *Nucleic Acids Res.* **40,** W117–W122 (2012).
51. Huang, P. *et al.* Heritable gene targeting in zebrafish using customized TALENs. *Nat. Biotechnol.* **29,** 699–700 (2011).
52. de la Motte, C. A. & Drazba, J. A. Viewing hyaluronan: imaging contributes to imagining new roles for this amazing matrix polymer. *J. Histochem. Cytochem.* **59,** 252–257 (2011).
53. Mann, K. D. *et al.* Cardiac response to startle stimuli in larval zebrafish: sympathetic and parasympathetic components. *Am. J. Physiol. Regul. Integr. Comp. Physiol.* **298,** R1288–R1297 (2010).
54. Schwerte, T., Prem, C., Mairösl, A. & Pelster, B. Development of the sympatho-vagal balance in the cardiovascular system in zebrafish (Danio rerio) characterized by power spectrum and classical signal analysis. *J Exp. Biol.* **209,** 1093–1100 (2006).
55. Letamendia, A. *et al.* Development and validation of an automated high-throughput system for Zebrafish *in vivo* screenings. *PLoS One* **7,** e36690 (2012).
56. Kopp, R., Pelster, B. & Schwerte, T. How does blood cell concentration modulate cardiovascular parameters in developing zebrafish (Danio rerio)? *Comp. Biochem. Physiol. A Mol. Integr. Physiol.* **146,** 400–407 (2007).
57. Kuhtreiber, W. M. & Jaffe, L. F. Detection of extracellular calcium gradients with a calcium-specific vibrating electrode. *J. Cell Biol.* **110,** 1565–1573 (1990).

Acknowledgements

We thank K.E. Yutzey for providing us the *pAC-CMV-Tbx5*, *Gal4-Tbx5-(266–518)*, *pAC-CMV-Tbx20*, *pMT2-GATA4* and *Gal4-VP16* expression plasmids; A. Kispert for providing us the reporter plasmid of *Tbx2(5.6/-0.316)-Luciferase*. We thank T. Wilson, M. Veldman and I. Bruce for language editing; Y. Gao, J. Zhang for lab management; Z. Jiang, J. Chen, X. Liu, J. Lu and G. Gomez for technical support; Y. Jia, J. Chen, H. Cui and X. Yang for zebrafish husbandry. This work was supported by grants from the National Natural Science Foundation of China (31110103904, 30871418 and 30730056), the 973 program (2012CB945101 and 2011CBA01000), China Scholarship Council of Ministry of Education (201206010116), Marine public welfare grant 201005022 and COMRA research grant DY125-15-T-03.

Author contributions

X.T., Y.Z., B.Z., J.C. and S.L. conceived and designed experiments; X.T., Y.Z., W.L. and L.Y. performed the positional cloning. Y.Z. and X.T. performed *in situ* hybridizations, rescue experiments and reporter assays. Y.Z., W.X. and S.H. performed TALEN experiments. Z.L., Y.Z. and J.Y. performed IP and IF. X.T., Y.Z., D.L., Z.Z., B.Z. and S.L. wrote the manuscript.

Additional information

Accession codes: Deep sequencing data has been deposited in Gene Expression Omnibus under accession number GSE53022.

Supplementary Information accompanies this paper at http://www.nature.com/naturecommunications

Competing financial interests: The authors declare no competing financial interests.

Reprints and permission information is available online at http://npg.nature.com/reprintsandpermissions/

How to cite this article: Tong, X. *et al.* Kctd10 regulates heart morphogenesis by repressing the transcriptional activity of Tbx5a in zebrafish. *Nat. Commun.* 5:3153 doi: 10.1038/ncomms4153 (2014).